98ES-145

Measuring Aqueous Humor Glucose Across Physiological Levels: NIR Raman Spectroscopy, Multivariate Analysis, Artificial Neural Networks, and Bayesian Probabilities

Michael C. Storrie-Lombardi and James L. Lambert
Jet Propulsion Laboratory, California Institute of Technology

Mark S. Borchert
Childrens Hospital University of Southern California

Akio Kimura, James Roseto, Richard J. Bing
Huntington Medical Research Institutes

Abstract

We have elicited a reliable Raman spectral signature for glucose in rabbit aqueous humor across mammalian physiological ranges in a rabbit model stressed by recent myocardial infarction. The technique employs near infrared Raman laser excitation at 785 nm, multivariate analysis, non-linear artificial neural networks and an offset spectra subtraction strategy. Aqueous humor glucose levels ranged from 37 to 323 mg/dL. Data were obtained in 80 uL samples to anticipate the volume constraints imposed by the human and rabbit anterior chamber of the eye. Total sample collection time was 10 seconds with total power delivered to sample of 30 Mw. Spectra generated from the aqueous humor were compared qualitatively to artificial aqueous samples and an excitation offset technique was devised to counteract broadband background noise partially obscuring the glucose signature. Feature extraction and data analysis were accomplished using second order Savitsky-Golay derivatives, linear multivariate analysis (partial least squares fit) and non-linear (artificial neural network) techniques. Predicted glucose levels correlated well with expected glucose concentration (R^2= 0.98, n=32) .

INTRODUCTION

Non-invasive measurement of glucose metabolism by any method (including optical spectroscopy techniques) remains an elusive goal. Blood and most excreted fluids contain numerous optically active and fluorescing substances capable of obscuring glucose spectral signatures. Aqueous humor (AH) filling the anterior chamber of the eye between the lens and the cornea, however, contains relatively few optically active molecules. These are primarily glucose, lactate, ascorbate, and urea.[1] Glucose concentration in AH appears linearly related to plasma glucose levels in animal studies and the rate constant for transport of glucose into AH from the plasma is not affected by diabetes.[2] Lactate and urea levels in AH appear to vary with blood levels, while ascorbate is concentrated in AH by active transport mechanisms. These facts, combined with a spectroscopically accessible location behind the relatively optically clear cornea make AH a reasonable site to attempt non-invasive analysis of glucose metabolism.

The potential for non-invasive estimation of blood glucose employing Raman spectroscopy on AH has been previously suggested.[3] Preliminary work has demonstrated that mixtures of the primary AH metabolites can be distinguished from one another in water solutions.[4] Techniques have been described to hopefully increase Raman sensitivity and allow the measurement of these metabolites at laser intensities commiserate with *in vivo* safety constraints.[5,6] Reliable measurement of glucose at physiologic levels and under physiological conditions with Raman spectroscopy has only recently been described.[7,8]

The goals of this study are to determine whether (1) Raman spectra extracted from rabbit aqueous humor can provide a reliable measure of glucose concentration across ranges commonly encountered in hypoglycemic, healthy, and diabetic states; (2) the obscuring effect of broadband background apparent in AH samples can be eliminated using a spectral excitation offset strategy in combination with multivariate and artificial neural network signal processing algorithms; and, (3) simple non-linear artificial neural network techniques can generate a Bayesian probability estimating the reliability of a single sample measurement.

MAIN SECTION

RAMAN SPECTROSCOPY - This vibrational spectroscopy technique is of considerable interest to the astrobiology community as a probe instrument for extraterrestrial detection of DNA and aromatic amino acids[9] and to the general medical community for the noninvasive *in vivo* detection of neoplastic tissue.[10] Raman spectral bands are considerably narrower than those produced in classical infrared spectral experiments, making possible much more specific signatures characterizing a target molecule. In addition, Raman excitation in the near infrared region (700-1300nm) encounters minimal fluorescence in most biological aqueous media.

We have known for the past fifty years that during a photon activating event, the majority of the photons incident on a target molecule scatter with unchanged frequency, while a small proportion (one in 10^9 photons) of light scatters with a shift in photon energy. This Raman shift occurs if photon energy transfers to (or from) the target molecule during an inelastic collision. The resulting vibrational spectra produced reveals both the state of the atomic nuclei and the chemical bonding within a molecule, as well as the interactions between the molecule and its local chemical environment.

Attempts to employ Raman techniques to directly measure glucose concentration in serum, plasma, and whole blood have met with encouraging success *in vitro*.[11,12,13] Unfortunately, efforts to utilize these techniques *in vivo* have met with considerable difficulty. Whole blood contains numerous Raman-active biological molecules. In aqueous humor (AH), the glucose signature competes against relatively few Raman-active substances. The four dominant, Raman-active molecules in AH are (concentrations are for rabbit AH) glucose (97 mg/dL), lactate (84 mg/dL), urea (36 mg/dL), and ascorbate (16 mg/dL). There is also a small amount of protein (26 mg/dL) capable of producing fluorescence activity in sufficient strength to diminish Raman signal to noise ratios. Raman spectra from AH specimens of rabbits and humans, as well as spectra obtained through fresh excised rabbit corneas, demonstrate detectable peaks of activity attributed to glucose, lactate, urea, amino acids; and proteins.[1] Extracting one or more of these components demands the use of multivariate analysis statistical techniques.

OFFSET TECHNIQUE - Initial pilot studies in our laboratory demonstrated that we could reliably detect physiological glucose levels in artificial aqueous humour solutions.[8] An artificial aqueous humor was designed to provide random fluctuations in concentration for the four major optically active AH components across a range of concentrations from 1/2 to 13X normal values for rabbit. Metabolite levels in this range can be seen in healthy subjects as well as in hypoglycemia and diabetes (glucose), renal failure (urea), and lactic acidosis (lactate). The analysates were dissolved in pH buffered physiological saline. Variation in the other three

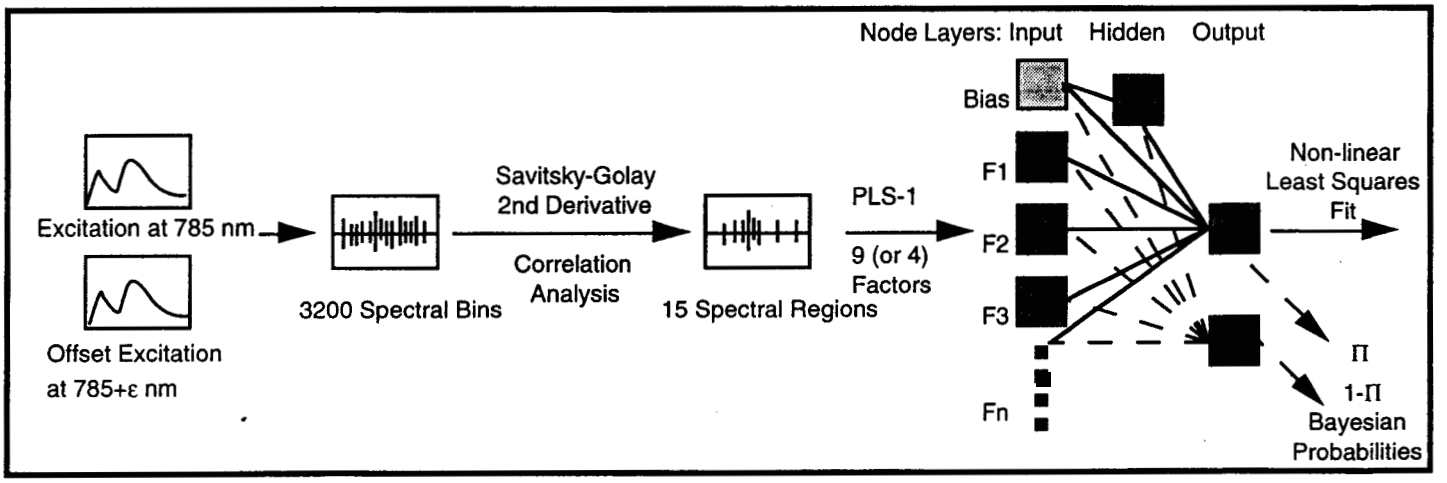

Figure 1. This flow chart for signal acquisition and processing depicts the production of Raman spectra with excitation at either 785nm or at an offset (785+ε), smoothing accomplished using a Savisky-Golay second derivative, determination of optimal correlation regions in the spectral set, and delivery of multifactor analysis output to the input layer of a non-linear ANN. The ANN configuration is the original backpropagation algorithm with linear feature extraction accomplished by the direct input from input nodes to output and the non-linear component extracted by a hidden layer node. In this case the final output produces a non-linear least squares fit to the data. The addition of a second output node and the creation of two discrete classes for glucose levels (e.g., normal and hyperglycemic) converts the algorithm to a Bayesian estimator. In this case the ANN calculates the probability that a particular vector belongs to either of the two classes.

analysates can dramatically alter glucose estimation. A multivariate analysis and neural network strategy adequately extracted the glucose signature from such solutions.

When glucose, lactate, ascorbate, and urea were mixed at concentrations approximating normal levels, the composite Raman signature evidenced marked similarity to that of the rabbit AH. However, the rabbit spectra also contained evidence of broadband fluorescence and elevated lactate activity.

Partial compensation for such activity can be obtained using standard first and second derivative techniques, such as the well-known Savitsky-Golay algorithm employed in this study. A more direct experimental approach of great utility involves acquiring two spectra for each sample. The first is obtained with an excitation frequency of, in our case, 785nm. The excitation wavelength is then offset slightly (with power adjusted to maintain a constant sample exposure). The offset is empirically determined to resolve the most prominent spectral line for the system. In our samples this was the urea line at 1002 cm^{-1}. The subtraction of these two spectra nulls the confounding broadband activity and converts true spectral peaks to biphasic signatures.

MUTIVARIATE ANALYSIS - The difficulties inherent in identifying and quantifying individual components of biological mixtures using Raman spectral analysis are well-documented and have spawned a wide variety of multivariate analysis techniques. For our multivariate algorithm we have chosen the partial least squares (PLS) technique, an analysis and spectral decomposition algorithm that, unlike principal component analysis (PCA), uses concentration information to calculate the eigenvectors.

In our design, test and training samples were put into a "round-robin" or autocorrellation training mode to iteratively employ all but one of the sample set in the minimization and eigenvector extraction process. Hence, the system trains on all but one of the samples, estimates the glucose level in that sample, then rotates the test sample back into the general pool and repeats the cycle until all samples have served as an unknown test subject. In this manner, the system is masked for the concentration of analysates in each unknown sample. PLS extracts only the linear interactions evident in a system. Since we know so little at this point about the precise interactions of the metabolites in AH particularly during pathological clinical states, a more general purpose and robust non-linear multivariate technique is required. Preliminary work in the laboratory of the senior author has demonstrated that certain artificial neural networks (ANNs) are a super-set of multivariate techniques and can elicit both linear and non-linear interactions. The factor scores generated by a multivariate analysis technique such as PLS or PCA can serve as the input vector to the ANN.

ARTIFICIAL NEURAL NETWORKS - ANNs such as the backpropagation algorithm, while originally modelled after biological systems, are actually best conceptualised and implemented as stochastic gradient descent search algorithms using a non-linear transfer function. Such an ANN can be proved a superset of classical signal processing techniques such as Fourier and multivariate analysis.[14] In a training sequence, ANN outputs are compared to known classifications using some cost function, often

$$E = 1/2\Sigma(o_K - \varepsilon_K)^2$$

During training, E is minimized with respect to the free parameters, the weights w_{ij}:

$$\Delta w_{ij}(t+1) = -\eta\, \delta E/\delta w_{ij} + \alpha \Delta w_{ij}(t)$$

where the learning coefficient, η, and the momentum, α, control the rate of learning (these depend primarily on data set size and the roughness of the solution landscape.

To train a network, we divide an initial data set into training vectors and test vectors. For small data sets it is best to sequentially pull a single vector for testing, train on the remainder, test against the unknown, and then iteratively repeat the process N times for a data set on N vectors. In this way every vector is tested without ever being seen by the algorithm during training. The total number of weights in the ANN, W, should be less than the total training set size N, ($W<N$). Larger networks will simply memorize the training set, act as a lookup table, and perform poorly when presented with novel samples. ANN output through a single node produces a non-linear least squares fit to the data In this study, the net trains against the predicted glucose levels using nine PLS factor scores and then estimates the unknown glucose level.

In this study we have employed the classical backpropagation configuration identified by Rumelhart, et al.[15] with the input nodes (plus a bias node) connecting both directly to the output node and indirectly via an intermediate hidden layer (see Figure 1). This configuration, often overlooked, simplifies analysis of the linear (input directly to output) and first order non-linear (input to hidden to output) contributions to the least squares fit. Specifically for this effort we employed an ANN with nine input nodes, a single node in the hidden layer, and a single output for a [9p;1,1] algorithm (where "p" denotes the connection of the prior or input layer directly to the output). Notice this configuration provides a total of 21 weights (9 input + 1 bias connected

to 1 hidden and 1 output, plus 1 weight connecting the hidden and output nodes).

Since the random initial setting of the weights make this a stochastic process, multiple restarts can provide statistical data on the accuracy of the output. In clinical usage it is critical that we supply an assessment of the reliability of a specific measurement. Such an estimate is often not available with statistical constraints only applying to the sample set as a whole and providing little information about a particular case. Multivariate analysis and the superset, artificial neural networks, provide techniques for acquiring this information. One such strategy employs an ANN to estimate the Bayesian probability of the correct classification of a sample vector into a discrete class of vectors, e.g. hypoglycemic, normal, or hypoglycemic.

BAYESIAN PROBABILITIES - ANN output can either be single node to provide a non-linear lest squares fit to a continuous dataset, or multi-nodal to provide discrete classifications. An ANN employed using a sigmoidal transfer function in 2-node output format produces the Bayesian *a posteriori* probability of correct classification.[16] For example, if the two nodes produce outputs of 0.9 and 0.1 for classes A and B, the ANN is reporting a 90% probability for the vector to be a member of class A. As a check of system function, note that the outputs should sum to 1. To illustrate the technique we modified the above ANN using four PLS factors as inputs to a [4p;1,2] network (see below).

EXPERIMENTAL METHODS - For our AH experiments we have chosen a Raman excitation wavelength in the near infrared region to diminish extraneous biological fluorescence and minimize tissue damage. The price for these advantages is a lower excitation efficiency since the Raman event exhibits an inverse relation between wavelength and excitation. Excitation at 785 nm was accomplished using a Spectra Physics model 2040E argon ion laser with an all lines mirror pumping a CW Ti:Sapphire solid state laser, Spectra Physics model 3900S.

The holographic probe head was mounted on an Olympus BX60 microscope with 10X objective. Data were collected using a Princeton Instruments MPP-type CCD camera with a 1024 by 256 array cooled with liquid nitrogen to -80 degrees C. This highly efficient camera and CCD recovers the efficiency loss due to increased wavelength. The system employs a Kaiser Optical Systems f/1.8 holographic imaging spectrograph with holographic filter and HoloPlex transmission grating.

As part of an ongoing investigation into nitric oxide metabolism and myocardium protection strategies, ten New Zealand white rabbits were sacrificed with a rapid exsanguination technique. These animals had experienced experimental myocardial infarction 48 hours prior to euthanasia and received 50-75 m/kg aspinol. Anesthesia included ketamine and xylazine. Rabbit AH was obtained from these animals within one minute of sacrifice. Rabbit AH samples were kept frozen until glucose levels could be measured and Raman spectroscopy performed. Glucose concentration in rabbit AH samples was measured with a commercial glucometer (Glucometer Elite®, Bayer) and confirmed against concentration standards.

Samples were placed in quartz cuvettes specifically designed to limit sample volume to 80 uL and to permit direct access to the test solution without traversing quartz walls or coverslips. Data acquisition and multivariate analysis were accomplished using Holograms® and Grams®, commercial software packages provided by Princeton Instruments and Galactic Industries Corporation, respectively. The integration time for each spectra was 10 seconds with an average power delivered to sample of 30mW. Spectra were first obtained using 785 nm excitation, then repeated after de-tuning the frequency sufficient to offset the pronounced spectral peak for urea ($1002cm^{-1}$) to produce a smooth biphasic signature while simultaneously nulling out the broadband interference.

A cross-correlational analysis of the original and offset spectra generated identified 15 regions correlating significantly ($R2>0.4$) with expected glucose concentration. This made it possible to implement a partial least squares algorithm for data reduction and calibration using fewer test measurements than data samples. This is particularly important when attempting to build a robust spectral prediction algorithm capable of iwithdtanding the effect of multi-metabolite concentration variance on spectral signatures. If a classification algorithm employs more test measurements (in our case, spectral bins) than data points, the algorithm will simply memorize the data and serve as a lookup table. The algorithm will correctly quantify the samples used to train it, but have poor results generalizing to new data sets. Our ability to identify a subset of spectral regions significantly correlated with metabolite concentration levels allowed us to decrease the number of input features from 3200 to less than the number of metabolite samples.

RESULTS AND DISCUSSION

To assess the capability of three signal processing strategies in a more nearly *in vivo* regimen, we lowered sample exposure time to 10 seconds and power delivered to sample to 30 mW. Special designed quartz cells, open to the Raman microscope probe, were employed to allow excitation of 80 uL volume of rabbit AH at 785nm, mimicking the geometric constraints imposed by an *in vivo* assay. AH samples were taken

within 10 to 60 seconds following experiment termination by cardiac extraction. The samples were then frozen for transport to our laboratory. Immediately prior to obtaining Raman signatures, the samples were warmed to room temperature and glucose levels, *[G]e*, measured using a Bayer Elite Clinical Glucometer. Figure 2 demonstrates the predictive ability of the current system.

For all three strategies we first examined the correlation coefficients for all spectral regions and identified 15 spectral regions with $R^2 > 0.4$ for use with PLS-1 during initial feature extraction. Such a strategy significantly diminished the degrees of freedom in the algorithm search from 3200 spectral bins to 389. Next, all spectra were smoothed using Savitsky-Golay second derivative across 49 points.

Figure 2a presents the outcome of using a single spectra for each sample (no offset technique and no ANN). This strategy produces a Raman spectral signature for glucose capable of predicting expected glucose concentration, *[Ge]*. Comparing the glucose concentration observed *[Go]* with the clinical glucometer results in a correlation coefficient, R^2 = 0.76 (n=32) across a range from 37 to 323 mg/dl (2a). Figure 2b shows the result of obtaining a second set of spectra by de-tuning from 785nm sufficient to shift Raman signatures the width of the prominent urea peak (power to sample was maintained at 30mW). This produces an excitation offset spectra. Subtraction of the primary and offset spectra results in a set of difference spectra capable of improving R^2 to 0.90. Finally, Figure 2c demonstrates the effect of using the offset spectra strategy and initial feature extraction by the linear PLS-1 algorithm, then employing a non-linear ANN to generate the final glucose estimate. In this case the correlation between *[Ge]*, and *[Go]* improves to 0.98.

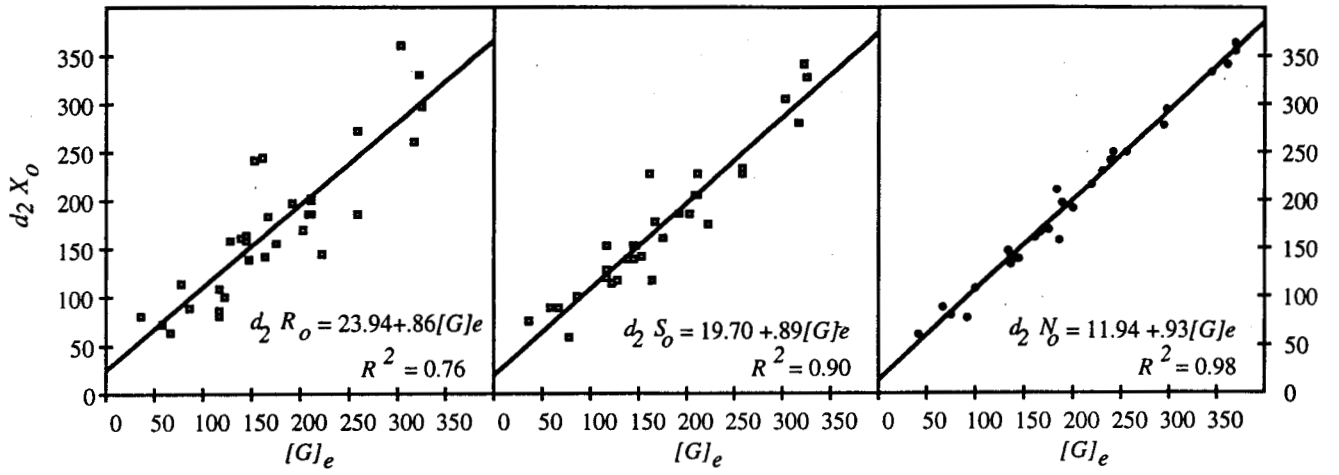

Figure 2. Excitation of 80 uL volume of rabbit AH at 785nm produces a Raman spectral signature for glucose capable of predicting expected glucose concentration ,*[Ge]*, with a Pearson correlation, R^2, of 0.76 (n=32) across a range from 37 to 323 mg/dl (Fig 2a). De-tuning from 785nm sufficient to shift Raman signatures the width of the prominent urea peak while maintaining power to sample at 30mW produces an excitation offset spectra. Subtraction of the primary and offset spectra results in a set of difference spectra capable of improving R^2 to 0.90. Figure 2c demonstrates the effect of using the offset spectra strategy and initial feature extraction by the linear PLS-1 algorithm, then employing a non-linear ANN to generate the final glucose estimate. In this case the correlation between *[Ge]*, and *[Go]* improves to 0.98. Collection time for each sample was 10 seconds and the resulting spectra were pre-processed using the Savitsky-Golay second derivative algorithm.

To increase the potential clinical utility of this system we investigated a strategy for assessing the reliability of a specific measurement. Recall that ANN output can either be single node to provide a non-linear lest squares fit to the dataset, or multi-nodal to provide discrete classifications. We reconfigured our ANN using a sigmoidal transfer function in 2-node output format to produce the Bayesian *a posteriori* probability of correct classification for a single sample into one of two discrete classes. To minimize the number of weights in this new network we determined that the first four PLS-1 factors provided better than 90% of the classification information. We constructed an ANN with four nodes in the input layer and a single node in the hidden layer resulting in a [4p;1,2] structure. The data set was arbitrarily divided into two sets with one containing 15 samples with glucose level *[Go]* < 160 mg/dL and the other set containing 17 samples with *[Go]* ≥ 160mg/dL. Note that it is important to keep the two classes approximately balanced for membership size. ANNs will extract BOTH vector difference information AND frequency distribution. This can be of great utility for large data sets comprising a significant sampling of real world data. For small data sets of indeterminate

samples with glucose level *[Go]* < 160 mg/dL and the other set containing 17 samples with *[Go]* ≥ 160mg/dL. Note that it is important to keep the two classes approximately balanced for membership size. ANNs will extract BOTH vector difference information AND frequency distribution. This can be of great utility for large data sets comprising a significant sampling of real world data. For small data sets of indeterminate frequency accuracy it will skew estimates significantly. Since we simply want to know how the ANN assess the features contained in a specific sample, we wish to minimize frequency information during these preliminary trials. Training and testing was again performed in autocorrelation mode with each test sample remaining unknown to the ANN during training.

The ANN agreed with the classification of 26 of 32 of the samples into the discrete high and low categories. As noted in earlier work in the laboratory of the senior author, the ANN probabilities in correct classifications (P_C) were higher than during incorrect classifications (P_i): $P_C = 0.72 \pm 0.14$, n=26; $P_i = 0.64 \pm 0.12$. Also as expected from a well-behaved system, the node outputs sum to 1. Three of the six classification discrepancies occur at the boundary region with *[Go]* = 145, 145, and 164 mg/dL and simply reflect sensitivity limits. However, three other anomalous vectors are far removed from the boundary with *[Go]* = 191, 209, and 223 mg/dL. Examination of these vectors revealed anomalies in the PLS-1 factors that clearly indicate the ANN correctly refused to classify these vectors as members of the higher glucose level set. In a clinical setting such a discrepancy would serve as an appreciated warning that the data need to be re-obtained to resolve the conflict.

CONCLUSION

In this study we have demonstrated (1) Raman spectra extracted from rabbit aqueous humor can provide a reliable measure of glucose concentration across ranges commonly encountered in hypoglycemic, healthy, and diabetic states; (2) the obscuring effect of broadband background apparent in AH samples can be eliminated using a spectral excitation offset strategy in combination with multivariate and artificial neural network signal processing algorithms; and, (3) simple non-linear artificial neural network techniques can generate a Bayesian probability estimating the reliability of a single sample measurement.

We find these initial results most encouraging and agree with others that Raman spectroscopy of aqueous humor in the near infrared combined with multifactor analysis techniques constitutes a new technology capable of estimating levels of blood glucose and perhaps other metabolites by non-invasive analysis of AH.

The rabbit AH signature in this initial study may also be complicated by the optical activity of the drugs introduced as part of surgical intervention and the cardiovascular experimental procedure. Potential Raman-active molecules include aspirin, ketamine, xylazine, pentobarbital, and heparin. We are currently investigating the Raman response of these and several other potentially confounding substances.

It is of note in passing but beyond the scope of this article, that our blood and AH glucose level measurements confirm the previously reported elevated glucose levels in rabbit AH in response to xylazine and is the subject of an ongoing investigation. Xylazine is commonly utilized in conjunction with ketamine as an anesthetic in veterinary surgical procedures. It appears to interfere with the release of insulin by pre-synaptic stimulation of alpha-2 receptors in the beta cells found in the Langerhans islets of the pancreas. This results in elevated blood glucose levels for two to six hours.[16]

We are currently proceeding to determine the minimum laser power and data acquisition time required for *in vivo* application. We expect that clinical utility of this methodology will require another order of magnitude reduction in power and integration time below current levels of 30mW and 10s. We suspect 1mW and 1s will be the gold standard for clinical acceptance of this technology. Studies are currently underway to elucidate the temporal correlation between glucose levels in AH and blood concentrations in a rabbit model.

ACKNOWLEDGEMENTS

The research described in this paper was partially performed at the Jet Propulsion Laboratory, California Institute of Technolgy under a contract with the Nattional Aeronautics and Space Administration. The authors gratefully acknowledge the support of this research by the Division of Life Sciences, National Aeronautics and Space Administration.

REFERENCES

1. Sears ML. Dynamics of ocular fluids and control of intraocular pressure: formation of aqueous humor, in Principles and Practice of Ophthalmology, Albert, DM and Jakobiec, FA (eds.) WB Saunders Co., Philadelphia, 1994.

2. DiMattio J. Decreased ascorbic acid entry into cornea of streptozotocin-diabetic rats and guinea-pigs, Exp. Eye Res. 55:337-344, 1992.

3. Tarr RV, and Steffes PG. Non-invasive blood glucose measurement system and method using stimulated Raman spectroscopy, U.S. Patent #5243983, Sept. 14, 1993.

4. Wang SY, Hasty CE, Watson PA, Wicksted RP, Stith, RD, and March WF. Analysis of metabolites in aqueous solutions

by using laser Raman spectroscopy, *Appl Optics* 32:925-929, 1993.

5. Wicksted JP, Erckens RJ, Motamedi M, and March WF. Raman spectroscopy studies of metabolic concentrations in aqueous solutions and aqueous humor specimens, *Appl Spect* 49:987-993, 1995.

6. Ozaki Y, Iriyama K, and Hamaguchi HO. Multichannel Raman spectroscopy of an intact lens: Raman measurement with laser irradiation below the threshold for retinal damage. *Appl Spect.* 41:1245-1247, 1987.

7. Storrie-Lombardi, MC, Lambert, J, and Borchert, M. Measuring glucose at physiological levels using near infrared Raman spectroscopy, multivariate analysis artificial neural networks, and Bayesian probabilities. Novel Technology Report NPO-20414/0012b, Jet Propulsion Laboratory, Pasadena, CA, 1997.

8. Lambert, JL, Storrie-Lombardi, MC, and Borchert, MS. Measuring glucose at physiological levels using near infrared Raman spectroscopy in artificial and rabbit aqueous humor, *LEOS* (in press).

9. Storrie-Lombardi, MC, Raman databases, Bayesian pattern matching, and non-linear artificial neural networks, JPL-Caltech *In Situ* Workshop on Raman Spectroscopy, June 6, Pasadena, CA, 1997.

10. Richards-Kortum, R and Sevickmuraca, E, Quantitative optical spectroscopy, Ann Rev Phys Chem 47, 555-606, 1997.

11. Dou, XM, Yamaguchi, Y, Yamamoto, H, Uenoyama, H and Ozaki, Y, Biological applications of anti-stokes-Raman spectroscopy - quantitative analysis of glucose in plasma and serum by a highly sensitive multichannel Raman spectrometer, *Appl Spect* 50(10):1301-6, 1996.

12. Berger, AJ, Itzkan, I, Feld, MS, Feasibility of measuring blood glucose concentration by near-infrared raman-spectroscopy, *Spectrochimica Acta Part A Molecular and Biomolecular Spectroscopy* 53(2):287-292, 1997.

13 Erckens, RJ, Motamedi, M, March, WF, Wicksted, J. Raman spectroscopy for noninvasive characterization of ocular tissue - potential for detection of biological molecules, *J Raman Spect* 28(5):293-9,1997.

14. Lahav, O, Naim, A, Sodré Jr, L, and Storrie-Lombardi, MC, Neural computation as a tool for galaxy classification: methods and examples, *Mon Not Roy Astro Soc*, 283(11), 207, 1996.

15. Rumelhart, DE, Hinton, GE, and Williams, RG, Learning representations by back-propagating errors, *Nature* 323 (6088), 533-6, 1986.

16. Storrie-Lombardi, MC, Lahav, O, Sodré, L, and Storrie-Lombardi, LJ, 1992, Morphological classification of galaxies by artificial neural networks, *Mon Not Roy Astro Soc* 259, 8-12.

17. Arnbjerg, J and Eriksen, T. Increased glucose content in the aqueous humour caused by the use of xylazine, *Opthal. Res.* 22:265-8,1990.